

**Calculational method to study the transmission properties of phononic crystals**

Zhilin Hou\* and Xiujun Fu

*Department of Physics, South China University of Technology, Guangzhou 510640, China*

Youyan Liu

*CCAST (World Laboratory), P.O. Box 8730, Beijing 100080, China**and Department of Physics, South China University of Technology, Guangzhou 510640, China*

(Received 20 November 2003; revised manuscript received 6 February 2004; published 28 July 2004)

An efficient numerical method is developed to calculate the transmission coefficient of the phononic crystals. By this method, the transmission properties of a two-dimensional phononic crystals constructed by the rectangle elastic isotropic lead rods embedded in uniform epoxy is investigated as an example. The transmission spectrum of the system is in excellent agreement with the band structure for the incident waves including both longitudinal and transverse polarized waves. The transmission spectra of the in-plane oblique incident waves are also calculated and discussed.

DOI: 10.1103/PhysRevB.70.014304

PACS number(s): 43.20.+g, 43.40.+s, 46.40.Cd

**I. INTRODUCTION**

The propagation of elastic or acoustic waves in periodic heterogeneous materials which is called phononic crystal has received much attentions in the last decade.<sup>1-19</sup> The existence of a full frequency gap in which the propagation of elastic waves is forbidden should have a potential application. Various systems with different materials (liquid and solid with different physical parameters) and inclusions (circular or rectangle rods for two-dimensional systems and sphere or cube for three-dimensional, etc.) have been investigated to enlarge the width of the full gap. To study the elastic wave behavior in this kind of system, several numerical analytical methods such as the plane-wave-expansion method (PWE),<sup>1-6</sup> the multi-scattering theory (MST),<sup>7-12</sup> and the finite-different time-domain method (FDTD)<sup>13-17</sup> have been developed and extensively used. Another method called the variational method (VM), which is based on the cubic B splines expansion, has been also developed recently.<sup>18,19</sup> Among them, the PWE method, by which the wave equations are solved in the Fourier space, is mostly used to calculate the band structure.

For the transmission properties of a finite system, the FDTD method and MST have been used by many researchers. The MST method, which is based on the Bessel function and(or) the Hankel function expansions, is very efficient and has good convergence. The waves in the system with spherical or elliptical boundary can be expressed by the Bessel and (or) Hankel function, which means the MST method can only be applied in the composite systems with spherical or elliptical shaped inclusions. The FDTD method is based on the real time simulation of the wave behavior; it can be used in the systems with any shaped inclusions. To obtain the transmission spectrum by this method, a fast Fourier transfer procedure on the simulation result has to be adopted, and no reflection coefficient could be defined.<sup>13,15</sup> Furthermore, when the system consists of materials with large contrast in their elastic properties, the FDTD method requires a very large number of discrete grids, which means a huge CPU time has to be consumed in the calculation.

In this paper, we present a calculating method of transmission spectrum, which is based on the eigenmode matching theory (EMMT). The basic idea is stemmed from the vector wave analysis of the surface grating.<sup>20,21</sup> By this method, the system is first cut into layers, waves in each layer are expressed as a superposition of basic function set, then the boundary condition is used to connect the nearest layers. Our results show that this method is very efficient to investigate the composite systems with rectangle shaped inclusions, which can not be treated by the MST method. This method can also be extended to study other composite systems with any shaped inclusions by selecting a suitable basic function set.

As an example of calculation, a two-dimensional phononic crystal which consists of square arranged parallel rectangular lead rods embedded in the epoxy matrix is investigated. The numerical result shows that the transmission spectra are in excellent agreement with the band structure for the incident wave including both longitudinal and transverse polarized waves. The transmission spectra of the in-plane oblique incident waves are also calculated and discussed.

This paper is organized as follows. In the next section we present the main idea and the formula of the EMMT method. In Sec. III, numerical results and discussions are given. We summarize the paper in Sec. IV.

**II. THEORY**

To show the EMMT method, we consider a two-dimensional phononic crystal with lattice constant  $a$  and filling fraction  $f=(2l/a)^2$  shown in Fig. 1, which is infinite in  $z$ - and  $x$ -directions, and have  $K$  total layers in the  $y$ -direction. As shown in the figure, we denote the considered system by layer labels  $1, 2, 3, \dots, K$  in the  $y$ -direction, where the uniform and composite layers are interlaced. The elastic plane wave is inputted from the left-most layer 1 and outgoing from the right-most layer  $K$ ;  $\theta$  is the in-plane incident angle.

The elastic wave propagating in elastic media can be described by

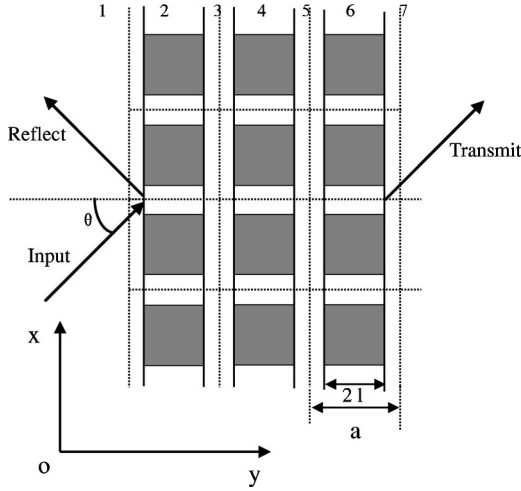


FIG. 1. Two-dimensional cross sections of the square array of parallel rectangular lead rods (shaded area) with edge length  $2l$  embedded in epoxy matrix. The system is infinite in  $x$  and  $z$  directions, the unit cell is shown by a dotted line, the solid line separates the system in the  $y$  direction into uniform and composite layers labeled  $1, \dots, 7$ ,  $\theta$  is the incident angle.  $a$  is the lattice constant.

$$\rho \frac{\partial^2 U_i}{\partial t^2} = T_{ij,i}, \quad (1)$$

$$T_{ij} = c_{ijkl} U_{k,l}, \quad (2)$$

where  $i, j, k, l = 1, 2, 3$ , respectively.

In a two-dimensional system, the  $xy$ -mode and  $z$ -mode can be decoupled, only the  $xy$ -mode in the phononic crystal can be excited when the incident waves have in-plane polarization. For this reason only the  $xy$ -mode will be considered in the following. Considering the elastic isotropy of the studied materials, Eqs. (1) and (2) can be simplified as<sup>22</sup>

$$\rho \omega^2 U_1 = (c_{11} U_{1,1} + c_{12} U_{2,2})_{,1} + T_{21,2}, \quad (3)$$

$$\rho \omega^2 U_2 = (c_{44} U_{1,2} + c_{44} U_{2,1})_{,1} + T_{22,2}, \quad (4)$$

$$T_{21} = c_{44} U_{1,2} + c_{44} U_{2,1}, \quad (5)$$

$$T_{22} = c_{12} U_{1,1} + c_{11} U_{2,2}, \quad (6)$$

where  $c_{11} = c_{12} + 2c_{44}$ .

In the uniform layers, the solution of Eqs. (3)–(6) can be written formally as a superposition of a set of perpendicular modes  $e^{j\alpha_n x}$

$$\begin{bmatrix} \mathbf{U} \\ j\mathbf{T}_2 \end{bmatrix} = \sum_{n=1}^N e^{i\alpha_n x} \left[ \sum_{r=1}^{2N} A_{rR} e^{j\beta_{rR} y} \begin{pmatrix} \mathbf{u}_{nR}^r \\ \mathbf{t}_{2nR}^r \end{pmatrix} + \sum_{r=1}^{2N} A_{rL} e^{j\beta_{rL} y} \begin{pmatrix} \mathbf{u}_{nL}^r \\ \mathbf{t}_{2nL}^r \end{pmatrix} \right] \quad (7)$$

with

$$\begin{aligned} \alpha_n &= \alpha_0 + nK \quad (n = 0, \pm 1, \pm 2, \dots, M), \\ \alpha_0 &= k_0 \sin \theta, \quad K = \frac{2\pi}{a}, \end{aligned} \quad (8)$$

$$\beta_{rR} = \begin{cases} \sqrt{k_l^2 - \alpha_n^2} & (rR = 1, \dots, N), \\ \sqrt{k_t^2 - \alpha_n^2} & (rR = N+1, \dots, 2N), \end{cases} \quad (9)$$

$$\beta_{rL} = \begin{cases} -\sqrt{k_l^2 - \alpha_n^2} & (rL = 1, \dots, N), \\ -\sqrt{k_t^2 - \alpha_n^2} & (rL = N+1, \dots, 2N), \end{cases} \quad (10)$$

where  $N = 2M + 1$  is the total term number of truncation.  $k_l = \omega/c_l$  with  $c_l = \sqrt{c_{11}/\rho}$ ,  $k_t = \omega/c_t$  with  $c_t = \sqrt{c_{44}/\rho}$  are the longitudinal and transverse wave vectors, respectively.  $\alpha_0$  is determined by the incident wave.  $\mathbf{U} = (U_1, U_2)^t$ ,  $j\mathbf{T}_2 = (jT_{21}, jT_{22})^t$ , and  $(\mathbf{u}_n^r, \mathbf{t}_{2n}^r)^t$  are the eigenvectors associated with  $\beta^r$ .

Equation (7) is also called the Rayleigh expansion of the wave,<sup>21</sup> in which the first term in the right-hand side denotes the left-forward wave, and the second corresponds the right-forward wave.

A matrix form of Eq. (7) is

$$\begin{pmatrix} \mathbf{U}^i \\ j\mathbf{T}_2^i \end{pmatrix} = \begin{pmatrix} e^{i\alpha x} & 0 & 0 & 0 \\ 0 & e^{i\alpha x} & 0 & 0 \\ 0 & 0 & e^{i\alpha x} & 0 \\ 0 & 0 & 0 & e^{i\alpha x} \end{pmatrix} \begin{pmatrix} u_R^i & u_L^i \\ t_{2R}^i & t_{2L}^i \end{pmatrix} \times \begin{pmatrix} e^{i\beta_R^i y} & 0 \\ 0 & e^{i\beta_L^i y} \end{pmatrix} \begin{pmatrix} A_R^i \\ A_L^i \end{pmatrix}, \quad (11)$$

where  $i$  is the layer label,  $e^{i\alpha x}$  is a  $N \times N$  diagonal matrix,  $e^{i\beta y}$  is a  $2N \times 2N$  diagonal matrix,  $u$  and  $t_2$  are the eigenvector matrix,  $A_R$  and  $A_L$  are the  $2N \times 1$  amplitude vectors corresponding to the right- and left-forward waves. In the inputting layer, which is labeled “1” in Fig. 1, we have  $A_R^1(m) = \delta_{m,1}$  for the longitudinal incident wave and  $A_R^1(m) = \delta_{m,N+1}$  for the transverse incident wave, where  $m$  means the  $m$ th component of  $A_R^1$ .

There are several ways to obtain the solution of Eqs. (3)–(6) in the composite layer. As a feasible way we first express the waves in each layer by the elementary functions, then use the boundary condition and Bloch theory to get the wave vectors  $\alpha$  and the related parameters  $\beta$ . This approach is more general but the calculation is more complicated. Another way is to expand the equation set into a Fourier series in the  $x$ -direction, and then obtain the mode of the  $y$ -direction by solving a scalar equation. In this paper, we work in the latter way for its simplicity.

A plane wave expansion of Eqs. (3)–(6) along the  $x$ -direction is

$$\begin{aligned} \sum_{G'} [-c_{11G-G'}(k+G)(k+G') + \omega^2 \rho_{G-G'}] U_{1k+G'} \\ = \beta \left[ \sum_{G'} c_{12G-G'}(k+G) U_{2k+G'} - jT_{21k+G} \right], \end{aligned}$$

$$\begin{aligned} \sum_{G'} [-c_{44G-G'}(k+G)(k+G') + \omega^2 \rho_{G-G'}] U_{2k+G'} \\ = \beta \left[ \sum_{G'} c_{44G-G'}(k+G) U_{1k+G'} - jT_{22k+G} \right], \end{aligned}$$

$$\begin{aligned}
 & - \sum_{G'} c_{44G-G'}(k+G')U_{2k+G'} - jT_{21k+G} \\
 & = \beta \left[ \sum_{G'} c_{44G-G'}(k+G)U_{1k+G'} \right], \\
 & - \sum_{G'} c_{12G-G'}(k+G')U_{1k+G'} - jT_{22k+G} \\
 & = \beta \left[ \sum_{G'} c_{11G-G'}(k+G)U_{2k+G'} \right], \quad (12)
 \end{aligned}$$

where  $G$  and  $G'$  take the values  $2\pi/a(-M, \dots, M)$ , which totally include  $N=2M+1$  terms;  $\beta$  is the wave vector along the  $y$ -direction.

Equation (12) gives a scalar equation about  $\beta$  with given frequency  $\omega$ . Solving the scalar equation,  $4N$  values of  $\beta$  and the corresponding  $4N$  eigenvectors can be obtained. To write out the wave solution in the composite layers as the form of Eq. (11), we have to separate the set of  $4N$  eigenvalues  $\sigma(\beta)$  into two subsets: The  $\sigma(\beta_R)$  is for the right-forward wave and the  $\sigma(\beta_L)$  for the left-forward wave. Generally,  $\sigma(\beta)$  consists of two distinct parts:  $\sigma = \sigma_1 + \sigma_2$ , where  $\sigma_1$  contains all of the real positive  $\beta$  and the complex ones with positive imaginary parts,  $\sigma_2$  contains all of the real negative  $\beta$  and the complex ones with negative imaginary parts, which correspond to the right-forward subset  $\sigma(\beta_R)$  and the left-forward subset  $\sigma(\beta_L)$ , respectively.

The boundary condition

$$\begin{pmatrix} \dot{\mathbf{U}}^{+i} \\ j\mathbf{T}_2^{+i} \end{pmatrix} = \begin{pmatrix} \dot{\mathbf{U}}^{-i+1} \\ j\mathbf{T}_2^{-i+1} \end{pmatrix}, \quad (13)$$

where the superscript  $+(-)i$  denotes the right (left) boundary of the  $i$ th layer, establishes the relationship between the  $i$ th and the  $i+1$ th layers.

Substituting the solutions, which have the form of Eq. (11), of the  $i$ th and  $i+1$ th layers into Eq. (13), by comparing the coefficients of each mode  $e^{j\alpha_n x}$  we get

$$u_R^i A_R^{+i} + u_L^i A_L^{+i} = u_R^{i+1} A_R^{-i+1} + u_L^{i+1} A_L^{-i+1}, \quad (14)$$

$$t_{2R}^i A_R^{+i} + t_{2L}^i A_L^{+i} = t_{2R}^{i+1} A_R^{-i+1} + t_{2L}^{i+1} A_L^{-i+1}. \quad (15)$$

To solve Eqs. (14) and (15), we define the reflection matrix  $R_+^i$ , the transmission matrix  $T^i$  and the general reflection matrix  $R_-^i$  as

$$A_L^{+i} = R_+^i A_R^{+i}, \quad (16)$$

$$A_R^{-i+1} = T^i A_R^i, \quad (17)$$

and

$$R_-^i = e^{-j\beta_L h_i} R_+^i e^{j\beta_R h_i}, \quad (18)$$

where  $h_i$  is the thickness of the  $i$ th layer, then Eqs. (14) and (15) can be rewritten as

$$\begin{pmatrix} u_R^i \\ t_{2R}^i \end{pmatrix} = \begin{pmatrix} u_R^{i+1} + u_L^{i+1} R_-^{i+1} & -u_L^i \\ t_{2R}^{i+1} + t_{2L}^{i+1} R_-^{i+1} & -t_{2L}^i \end{pmatrix} \begin{pmatrix} T^i \\ R_+^i \end{pmatrix}. \quad (19)$$

Note that the general reflection matrix  $R_-^K$  in the outputting layer equals zero, and the amplitude of incident wave  $A_R^1$  on the left-most layer is known; the reflection and transmission matrix of each layer can be obtained by repeatedly using Eq. (19).

So the reflecting, transmitting, and incident waves can be expressed as

$$\begin{pmatrix} \mathbf{U}^{\text{ref}} \\ j\mathbf{T}_2^{\text{ref}} \end{pmatrix} = \begin{pmatrix} \mathbf{u}_L^1 \\ \mathbf{t}_{2L}^1 \end{pmatrix} R_+^1 A_R^1, \quad (20)$$

$$\begin{pmatrix} \mathbf{U}^{\text{tra}} \\ j\mathbf{T}_2^{\text{tra}} \end{pmatrix} = \begin{pmatrix} \mathbf{u}_R^N \\ \mathbf{t}_{2R}^N \end{pmatrix} T^{\text{total}} A_R^1, \quad (21)$$

and

$$\begin{pmatrix} \mathbf{U}^{\text{in}} \\ j\mathbf{T}_2^{\text{in}} \end{pmatrix} = \begin{pmatrix} \mathbf{u}_R^1 \\ \mathbf{t}_{2R}^1 \end{pmatrix} A_R^1, \quad (22)$$

where  $T^{\text{total}} = T^K e^{i\beta_R^K} \dots T^1$  is the total transmission matrix.

Reflection coefficient can be defined as the ratio of average reflecting energy flux and the average inputting energy flux along the  $y$ -direction

$$R = \frac{\sum_{i=1}^{2N} \text{real}[(\dot{U}_i^{\text{ref}})^* T_{2i}^{\text{ref}}]}{\sum_{i=1}^{2N} \text{real}[(\dot{U}_i^{\text{in}})^* T_{2i}^{\text{in}}]}. \quad (23)$$

In the same way, we can define the transmission coefficient as

$$T = \frac{\sum_{i=1}^{2N} \text{real}[(\dot{U}_i^{\text{tra}})^* T_{2i}^{\text{tra}}]}{\sum_{i=1}^{2N} \text{real}[(\dot{U}_i^{\text{in}})^* T_{2i}^{\text{in}}]}, \quad (24)$$

where  $(\dot{U}_i)^*$  means the conjugate of the  $i$ th component of the vector  $\dot{U}$ , and ‘‘real’’ is a operation deriving the real part of a complex value. Energy conservation condition  $T+R=1$  should be expected in the calculation procedure.

### III. RESULT AND DISCUSSION

As an example, we use the above EMMT method to investigate the transmission property of the system shown schematically in Fig. 1. In the figure, the embedded material is elastic isotropic rectangular lead rods with parameters  $\rho = 11\,400 \text{ Kg/m}^3$ ,  $c_l = 2160 \text{ m/s}$ ,  $c_t = 860 \text{ m/s}$ , the background material is epoxy with  $\rho = 1180 \text{ Kg/m}^3$ ,  $c_l = 2535 \text{ m/s}$ ,  $c_t = 1157 \text{ m/s}$ . The transmission coefficients of the system with 40 layers along the  $y$ -direction (including 20 unit cells) are investigated, 17 plane waves ( $G = -8, \dots, +8$ ) are used to expand  $\mathbf{U}$  and  $\mathbf{T}_2$  along the  $x$ -direction. For

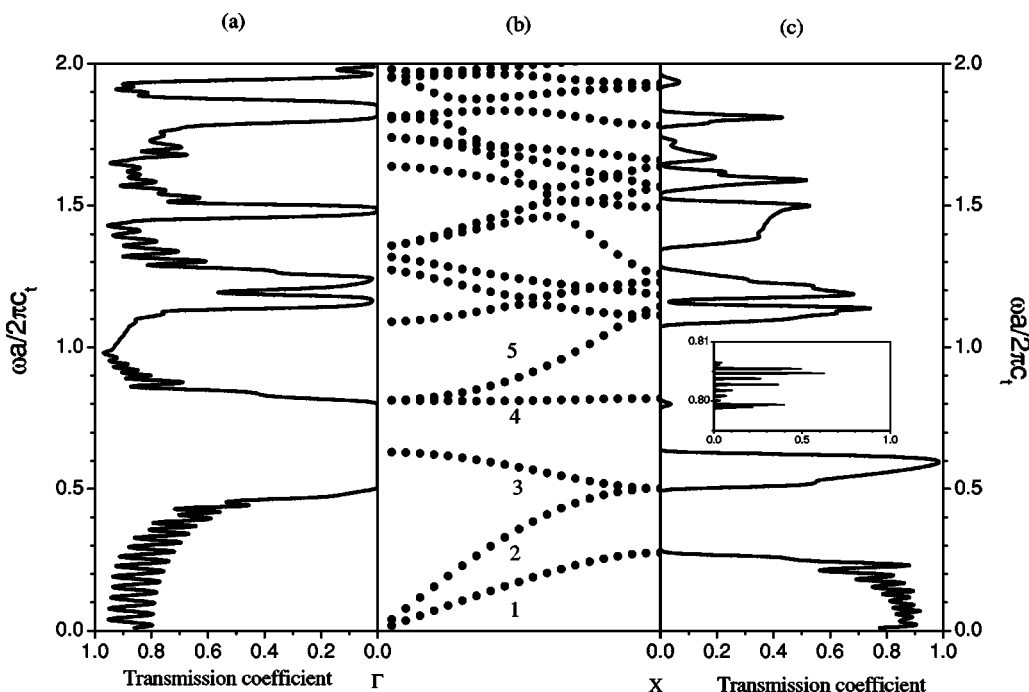


FIG. 2. The transmission spectra with filling fraction  $f=0.16(2l/a=0.4)$  and  $\theta=0$ . The frequency is scaled as  $\omega a/2\pi c_t$ , where  $c_t$  is the velocity of the transverse wave in epoxy. In the figure, (a) for the longitudinal polarized incident wave, (c) for the transverse polarized incident wave, the inset in (c) shows the transmission spectrum around  $\omega a/2\pi=0.8$  of (c). (b) Shows the band structure of the system along  $\Gamma X$  direction of the first SBZ. Arabic numerals in (b) label the bands.

comparable convenience, the band structure of the system is also calculated by using the PWE method with  $G_x, G_y = -8, \dots, +8$ ; 289 plane waves in total. All the computation is strictly controlled under the condition  $R+T=1\pm 1.0\times 10^{-8}$ . We would like to point out that this adopted method is very efficient and powerful, less than a half second (by the PC with Pentium IV 1.7G CPU and 512M byte SDR RAM) is needed for one  $\omega$  do-loop.

As some previous works pointed out,<sup>8,18</sup> the transmission spectrum strongly depends on the polarization of the incident wave, longitudinal and transverse polarized incident waves would give different transmission spectrum. To display this point we present the transmission spectra of the longitudinal polarized incident wave and transverse polarized incident wave with incident angle  $\theta=0$  and filling fraction  $f=0.16$  in Figs. 2(a) and 2(c), respectively. Figure 2(b) is the band structure of the studied system along the  $\Gamma X$  direction, from which we see that some permitted bands shown in Fig 2(b) do not have corresponding nonzero transmission region, such as the third and fourth band labeled in Fig. 2(b) for Fig. 2(a) and the second and the fifth bands in Fig. 2(b) for Fig. 2(c). The physical origin of it should be that not all of the modes in the composite material can be excited by the single polarized incident wave, which leads to a zero transmission coefficient region in the spectrum. A superposition of these two spectra is plotted in Fig. 3(a), which shows excellent agreement with the band structure. This means that the permitted bands of the phononic crystal can be separated into two parts, one associates with the longitudinal polarized wave and the other one associates with the transverse polarized wave. On the other hand, the transmission spectrum of the mixed incident wave including both longitudinal and trans-

verse polarized waves can be obtained by setting the amplitude of incident wave

$$A_R^1 = (\overbrace{1, 0, \dots, 0}^N, \overbrace{1, 0, \dots, 0}^N)$$

For this case, the numerical result is shown in Fig. 3(c), where we can see that the spectrum shows the same profile as Fig. 3(a).

We have also calculated the transmission spectrum of the same system with filling fraction  $f=0.64$  and  $\theta=0$ . The numerical results are shown in Fig. 4, with Fig. 4(a) showing the superposition of the transmission coefficients of both longitudinal and transverse polarized incident waves and Fig. 4(c) showing the transmission spectrum of the mixed incident wave. Figure 4(b) displays the band structure of the system along the  $\Gamma X$  direction. These results support again our above conclusions.

Another point we would like to state is that the presented EMMT method can also be used to calculate the transmission spectra of the incident waves with  $\theta \neq 0$ , which means  $\alpha_0 \neq 0$  in Eq. (8) except  $\omega=0$ . The results of a system with  $f=0.64$  and  $\theta=45^\circ$  is presented in Fig. 5, where Fig. 5(a) is the spectrum for longitudinal incident waves, Fig. 5(c) for transverse incident waves, and Fig. 5(b) shows the band structures along the  $\overline{XM}$  and  $\overline{M\Gamma}$  directions of the first SBZ (surface Brillouin zone) of the system. From them ones can see that the band gaps existing in Fig. 5(b) coincide with the zero-transmission-coefficient region of Figs. 5(a) and 5(c) very well. One may note that both of the transmission spectra for longitudinal and transverse polarized incident waves shown in Figs. 5(a) and 5(c) drastically fluctuate with the

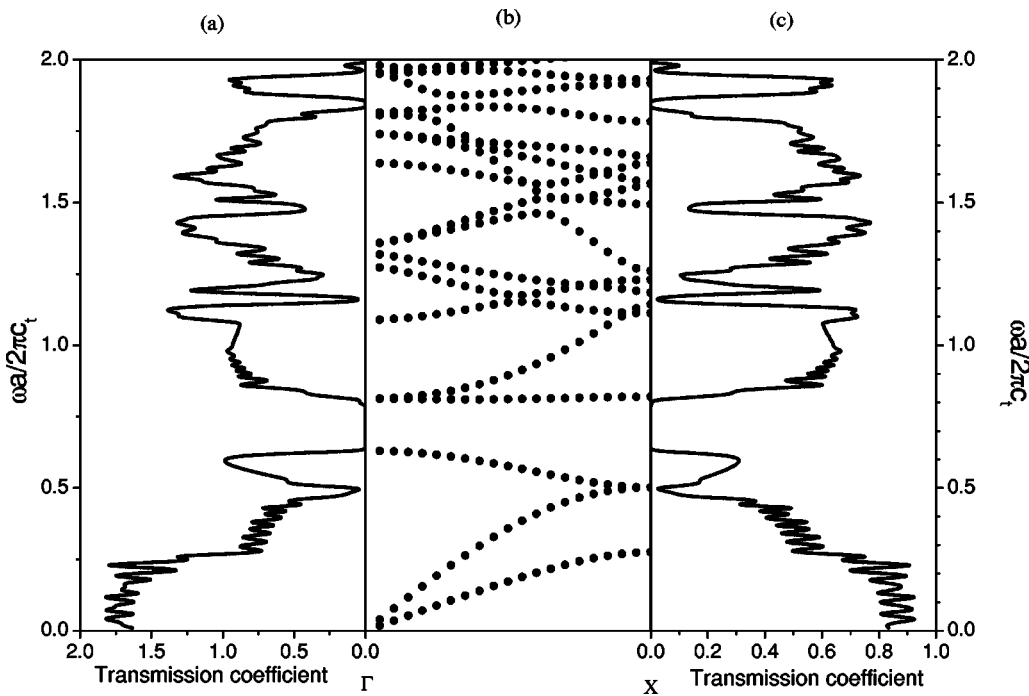


FIG. 3. The transmission spectra with filling fraction  $f=0.16(2l/a=0.4)$  and  $\theta=0$ . (a) a simple superposition of Figs. 2(a) and 2(c). Results for the incident wave including both longitudinal and transverse polarized waves. (b) Band structure along  $\Gamma X$  direction of the first SBZ.

frequency of the incident wave increasing, the reason is that an incident wave with a nonzero incident angle  $\theta$  can excite not only longitudinal but also transverse associated modes in the phononic crystal. Another point we have to point out is that we can not give a band structure along a certain direction of the SBZ, which directly corresponds to the spectra of the incident waves with a regular nonzero incident angle, the

bands along  $\overline{XM}$  and  $\overline{M\Gamma}$  presented in Fig. 5(b) just show that corresponding to the band gaps the transmission coefficients are zero. The reason to calculate this spectra is that it can be easily obtained and can be easily realized in practice.

Finally, we would like to point out that the presented EMMT method can be easily extended to deal with the liquid-solid composite systems consisted of the materials

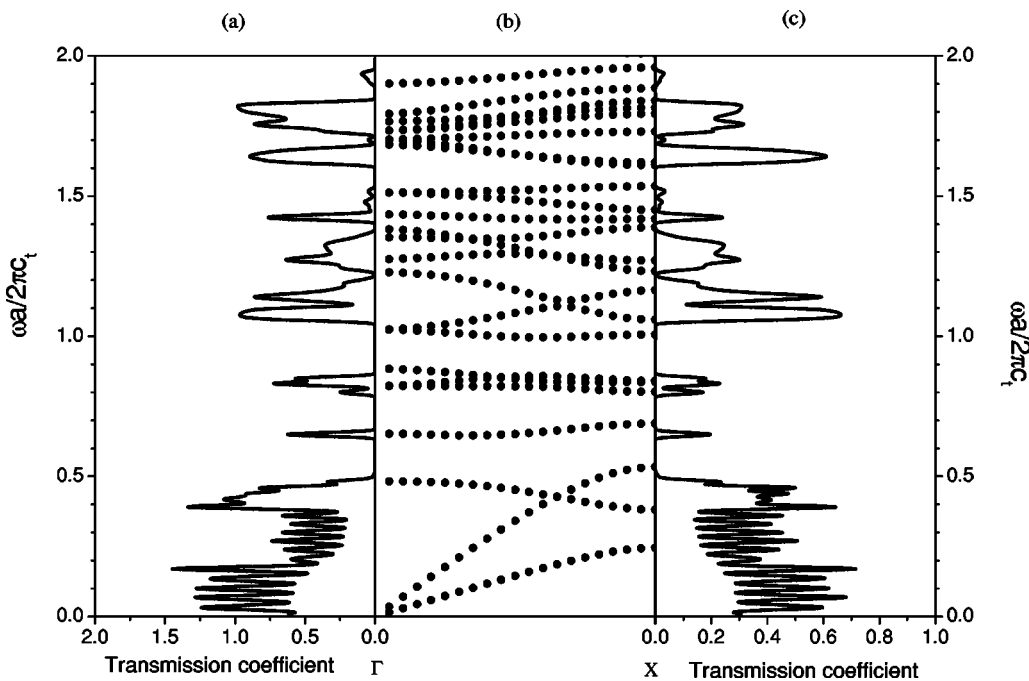


FIG. 4. Same as Fig. 3 with filling fraction  $f=0.64(2l/a=0.8)$ .



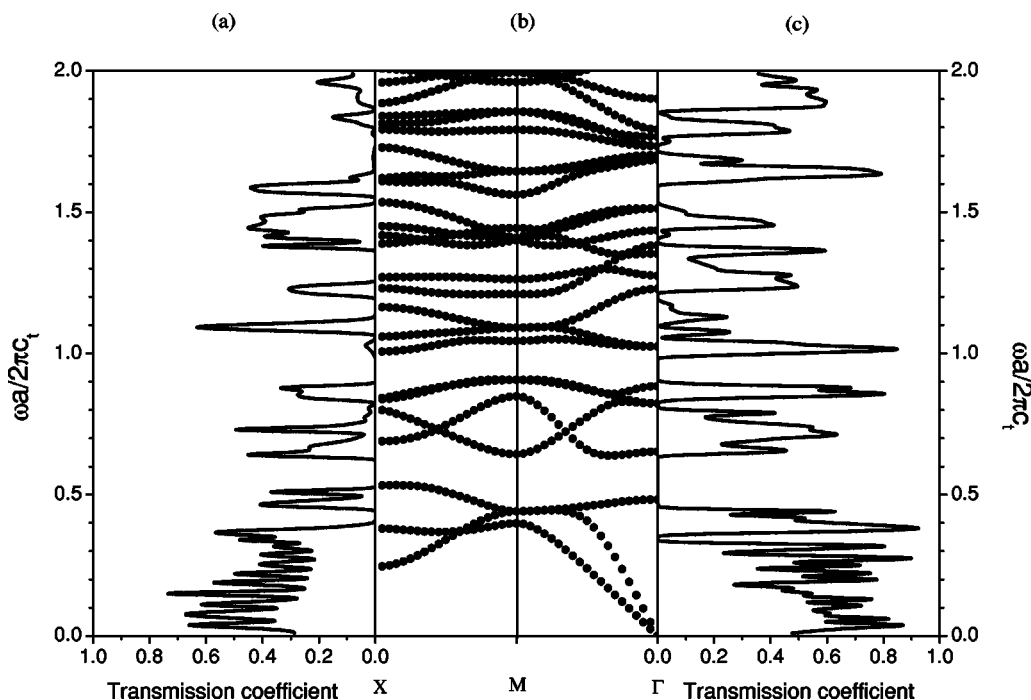


FIG. 5. The transmission spectra of the system with filling fraction  $f=0.64$  and  $\theta=45^\circ$ . (a) Corresponds to the longitudinal polarized incident wave. (c) Corresponds to the transverse polarized incident wave. (b) Band structure of the system along  $\overline{XM}$  and  $\overline{M\Gamma}$  direction of the first SBZ.

with elastic constants independent of frequency. In fact, instead of the plane wave expansion, the wave solution in layers can be obtained by first expressing the waves in each unit cell with elementary functions and then using boundary condition in  $x$  direction. For other more complicated systems, such as the composite system with circular inclusion, the transmission coefficient can also be investigated by the present method, what we need is to cut the inclusions into thin parallel slices.

#### IV. BRIEF SUMMARY

A calculation technique, the eigenmode matching theory (EMMT), is developed to examine the transmission property of the phononic crystals with rectangular shaped isotropic elements embedded in uniform materials. A two-dimensional

epoxy-lead system is investigated by the presented method, the numerical results show excellent agreement between the phononic band structure and transmission spectrum when the in-plane direct incident wave includes both of longitudinal and transverse polarized waves. The transmission properties of the same system with single longitudinal or transverse in-plane oblique incident waves are also investigated and discussed. The calculating procedure shows that this method is very efficient for the materials with elastic constant independent of the frequency.

#### ACKNOWLEDGMENTS

This work was supported by the National Natural Science Foundation of China under Grant No. 90103027 and Guangdong Provincial Natural Science Foundation of China under Grant No. 013009.

\*Electronic address: phzhou@scut.edu.cn

<sup>1</sup>Toshio Suzuki and Paul K. L. Yu, *J. Mech. Phys. Solids* **46**, 115 (1997).

<sup>2</sup>Fugen Wu, Zhilin Hou, Zhengyou Liu, and Youyan Liu, *Solid State Commun.* **123**, 239 (2002).

<sup>3</sup>Zhilin Hou, Xiujun Fu, and Youyan Liu, *Phys. Lett. A* **317**, 127 (2003).

<sup>4</sup>C. Goffaux and J. P. Vigneron, *Phys. Rev. B* **64**, 075118 (2001).

<sup>5</sup>Fugen Wu, Zhengyou Liu, and Youyan Liu, *Phys. Rev. E* **66**, 046628 (2002).

<sup>6</sup>Xin Zhang, Zhengyou Liu, Youyan Liu, and Fugen Wu, *Phys.*

*Lett. A* **313**, 455 (2003).

<sup>7</sup>Zhengyou Liu, C. T. Chan, Ping Sheng, A. L. Goertzen, and J. H. Page, *Phys. Rev. B* **62**, 2446 (2000).

<sup>8</sup>I. E. Psarobas, N. Stefanou, and A. Modinos, *Phys. Rev. B* **62**, 278 (2000).

<sup>9</sup>Zhengyou Liu, Xingiang Zhang, Yiwei Mao, Y. Y. Zhu, Zhiyu Yang, C. T. Chan, and Ping Sheng, *Science* **289**, 1734 (2000).

<sup>10</sup>I. E. Psarobas and M. M. Sigalas, *Phys. Rev. B* **66**, 052302 (2002).

<sup>11</sup>Lorenzo Sanchis, Andreas Hakansson Francisco Cervera, and Jose Sanchez-Dehesa, *Phys. Rev. B* **67**, 035422 (2003).

- <sup>12</sup>M. Kafesaki and E. N. Economou, Phys. Rev. B **60**, 11993 (1999).
- <sup>13</sup>J. O. Vasseur, P. A. Deymier, A. khelif, Ph. Lambin, B. Djafari-Rouhani, A. Akjouj, L. Dobrzynski, N. Fettouhi, and J. Zemmouri, Phys. Rev. E **65**, 056608 (2002).
- <sup>14</sup>Yukihiro Tanaka, Yoshinobu Tomoyasu, and Shin-ichiro Tamura, Phys. Rev. B **62**, 7387 (2002).
- <sup>15</sup>Ph. Lambin, A. Khelif, J. O. Vasseur, L. Dobrzynski, and B. Djafari-Rouhani, Phys. Rev. E **63**, 066605 (2001).
- <sup>16</sup>M. M. Sigalas and N. Garcia, Appl. Phys. Lett. **76**, 2307 (2000).
- <sup>17</sup>D. Garcia-Pablos, M. Sigalas, F. R. Montero de Espinosa, M. Torres, M. Kafesaki, and N. Garcia, Phys. Rev. Lett. **84**, 4349 (2000).
- <sup>18</sup>J. V. Sanchez-Perez, D. Caballero, R. Martinez-Sala, C. Rubio, J. Sanchez-Dehesa, F. Meseguer, J. Linares, and F. Galvez, Phys. Rev. Lett. **80**, 5325 (1998).
- <sup>19</sup>Cecile Goffaux and Jose Sanchez-Dehesa, Phys. Rev. B **67**, 144301 (2003).
- <sup>20</sup>Li Lifeng, J. Opt. Soc. Am. A **13**, 1024 (1996).
- <sup>21</sup>Li Lifeng, J. Mod. Opt. **45**, 1313 (1998).
- <sup>22</sup>Mikael Wilm, Sylvain Ballandras, Vincent Laude, and Thomas Pastureaud, J. Acoust. Soc. Am. **112**, 943 (2002).